[MEET THE EXPERT]
IMPLANTS

Materials and Surface Technology for Implants

Thursday, 8th September 2022

FHNW Campus Muttenz
Hofackerstrasse 30
4132 Muttenz / Switzerland

Conference Documentation

Main organizer

RMS — Testing · Research · Consulting

www.rms-foundation.ch

Sponsors

STEIGER Galvanotechnique SA

MOTOREX® Oil of Switzerland

KKS — Experts in Surface Treatment & Ultrasonic Cleaning

mps MICROSYSTEMS

GLOOR INSTRUMENTS
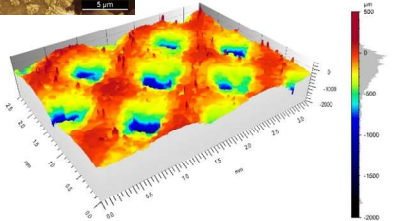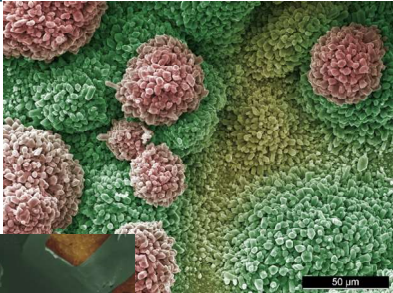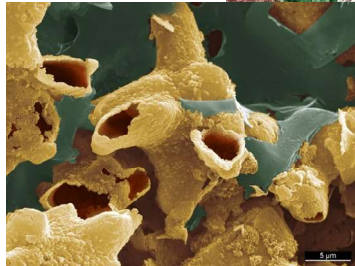
Main Organizer

RMS Foundation, Bettlach, Switzerland

Testing, consulting and technology transfer …
… in medical and materials technologies

➢ Qualification of raw materials …
   … validation and control of production processes …
      … feedback and failure analysis

➢ Newer and special services:
   - Chemical and particulate contaminations
   - Leachables and extractables
   - Validation of cleaning procedures
   - Packaging systems
   - Qualification of additive manufacturing
   - Functional and dynamic testing

ISO 9001 certification and **ISO 17025** accreditation

Sponsors

Partner
SWISS MEDTECH

General Information

Venue

FHNW Campus Muttenz
Hofackerstrasse 30
4132 Muttenz / Switzerland

Exhibition, breaks, catering: **Aula, ground floor**
Sessions: **Auditorium 02.W.18**

Powerpoint presentations

The PowerPoint Presentations shown at this event remain in the property of the authors and presenters. The organizer will not distribute the presentations. Please contact the corresponding author if you wish to receive more information on a specific presentation. E-Mail addresses of the authors can be found on the list of authors on page 30 of this documentation.

Audio recording and use of cameras

Audio recording and the use of cameras (photo and video) is not allowed during the sessions. Please contact the corresponding author if you wish to receive more information on a specific presentation. E-Mail addresses of the authors can be found on the list of authors at the end of this documentation.

Publication

All abstracts that qualify will be published online in a Conference Collection of the eCM Conferences Open Access online periodical. Please register on the eCM Conferences site for paper notification: http://ecmconferences.org/

Pdf-File of this conference documentation

The pdf version of this documentation as well as the documentations of past conferences are published on the website of the RMS Foundation:

https://www.rms-foundation.ch/en/mte-conference

Feedback

There will be no comment form. If you would like to give us feedback, be it recognition or suggestions for improvement, please send an e-mail to Lukas.Eschbach@rms-foundation.ch
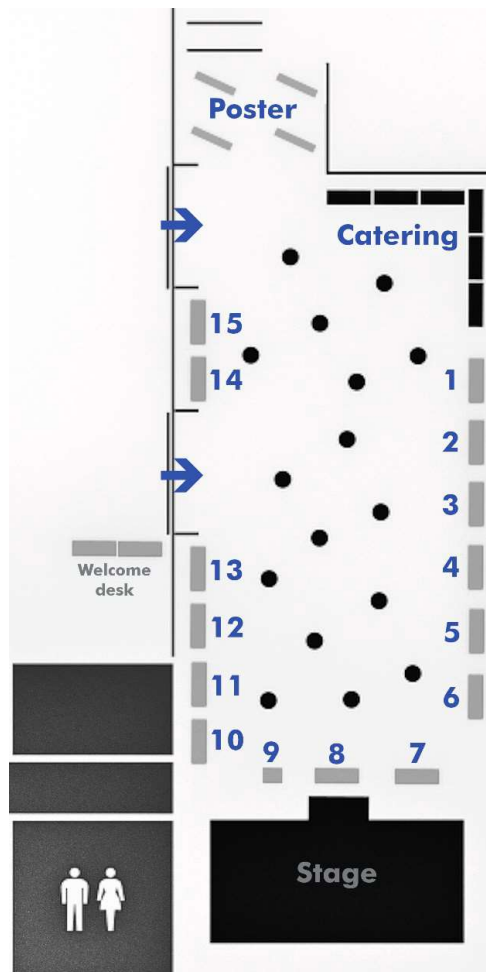
Badge return

Please leave your badge in the recycling box at the exit after the event.

Exhibition area and list of exhibitors

1	MOTOREX AG LANGENTHAL
2	KKS Ultraschall AG
3	MPS Micro Precision Systems AG
4	Steiger Galvanotechnique SA
5	Gloor Instruments AG
6	Carl Zeiss AG
7	RMS Foundation
8	ORTHOMANUFACTURE - Epic sarl
9	Innovation Booster - Microtech
10	Medicoat AG
11	FHNW
12	Namsa Clinical & Consulting GmbH
13	Rösler Schweiz AG
14	Swiss m4m Center
15	

Sponsors of [MEET THE EXPERT] Implants 2022

Sponsors of [MEET THE EXPERT] Implants 2022

Sponsors of [MEET THE EXPERT] Implants 2022

Meeting Program Thursday 8ᵗʰ September 2022

08:30	**Registration / Welcome Coffee**
09:00-09:15	Welcome message
	Session 1 Chairperson: **Lukas Eschbach**
09:15-09:45	Keynote 1: Prof. Dr. Konrad Wegener, Inst. f. Werkzeugmaschinen, ETHZ, CH: *AI for Autonomy in Manufacturing*
09:45-10:30	Flash Presentations Exhibitors and Posters (1 min. each)
10:30-11:00	Break (Exhibition and Poster)
	Session 2: *Additive Manufacturing* Chairperson: **Michael de Wild**
11:00-11:30	Keynote 2: PD Dr. med. et med. dent. Florian M. Thieringer, Univ. Hospital Basel, CH: *3D-Printed PEEK implants: clinical needs & point of care production*
11:30-11:50	Jürgen Wuttig, Sauber Technologies AG, Hinwil, CH: *Microstructure of HIPped SLM-Ti-6Al-4V*
11:50-12:10	Dr. Juliane Thielsch, Fraunhofer Inst. for Machine Tools and Forming Techn. IWU, Dresden, DE: *Implants with complex open-pored cellular structure additively manufactured by LPBF using geometry adapted slicing functions*
12:10-12:30	Dr. Dmitrii Komissarenko, EMPA, Dübendorf, CH: *Additive manufacturing of zirconia canine elbow joint implants via digital light processing*
12:30-13:50	Lunch (Exhibition and Poster)
	Session 3: *Materials and Surfaces* Chairperson: **Simon Berner**
13:50-14:10	Dr. Dieter Ulrich, Helbling Technik, Liebefeld-Bern, CH: *Wireless Power Transfer for "Smart" Implants*
14:10-14:30	Dr. Samuel Rey-Mermet, HES-SO Valais, Sion, CH: *Additively manufactured Nitinol stent: surface finish and properties*
14:30-14:50	Dr. Oksana Banakh, Haute Ecole Arc, La Chaux-de-Fonds, CH: *Micro-arc anodized magnesium AZ31 alloy: towards application in veterinary implants*
14:50-15:10	Harald Holeczek, Medicoat AG, Mägenwil, CH: *Anti-bacterial coating for implant surfaces based on electrochemically-formed $Ca(OH)_2$*
15:10-15:40	Break (Exhibition and Poster)
	Session 4: *Clinical and Regulatory Topics* Chairperson: **Christiane Jung**
15:40-16:10	Keynote 3: PD Dr. med. Dr. phil. Andrej M. Nowakowski, Kantonsspital Baselland, CH: *Challenges in revision total hip replacement and prosthetic joint infections*
16:10-16:30	Christoph Sprecher, AO Research Institute, Davos, CH: *Artificially induced peri-implant inflammation around mechanically loaded Zirconia and Titanium implants*
16:30-16:50	Helen Yau, Koln 3D Switzerland, Geneva, CH: *Clinical Applications of Patient-Specific Implants: How to Avoid Reinventing the Wheel*
16:50-17:10	Sanja Savic, OFI Technologie & Innovation GmbH, Vienna, AT: *Challenges and in-vitro solutions for the biocompatibility assessment with chemical characterization based on ISO 10993*
17:10-17:30	Dr. Hans Schmotzer, SigmaRC GmbH, Cham, CH: *In vitro testing of degradable magnesium implants – Avoiding the pitfalls*
17:30-17:40	Roundup

AI for Autonomy in Manufacturing

K. Wegener[1,2]

[1]Institut für Werkzeugmaschinen und Fertigung (IWF) ETH Zürich, CH,
[2]inspire AG, Zürich, CH

INTRODUCTION: With the new paradigms in manufacturing of industrie 4.0 and biological transformation, massive changes will challenge the manufacturing industry and huge benefits will be the recompensation of a successful transformation. Zero fault production, increase of machine autonomy and reliability, increase of quality even for complicated manufacturing tasks with less complexity towards the operator are the goals of this transformation. Complicated processes as for instance additive manufacturing at the border of manufacturability and simplification towards the machine user, leaves only the described development vector.

CONCEPT: The vision "operator integrated" is shown in Fig. 1 for a machine for laser powderbed fusion (LPBF). LPBF is a process that is dominated by a few process parameters, but depends on estimated 200 parameters that are only partly controlled. It is thus the typical complex process, and a generalized CAM-tool as for milling processes does not exist. The concept of biological transformation seeks to find technical solutions by inspiration from biology, by integrating biological elements and by utilizing information technology for an intelligent way of production.
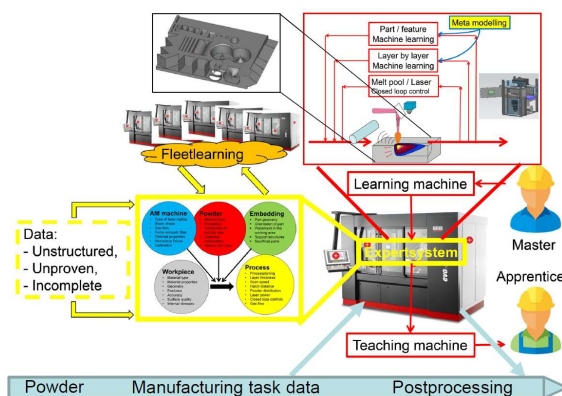
Fig. 1: Vision "operator integrated" as solution for complex manufacturing process additive manufacturing [1].

Similar concepts can be rolled out to actually all manufacturing processes and their machines. Essential is the utilization and integration of diverse bidirectional information streams from and to the manufacturing execution system (MES), other machines, the process, the machine status, and equally important to users with different skill sets. Novelty is the level of monitoring with full field and fused sensors together with intelligent data processing the teaming and communication with human operators and the vault of experience represented by a self-learning expert system on the basis of ontologies.

REALISATION STEPS: Different partial solutions for the concept can be shown as examples: The prerequisite for all data transfer with MES-systems and other machines for federated or transfer learning is the realization of machine connectivity, which is shown for different situations taking also legacy machines into account. Data processing filtering out necessary information is a huge challenge, but the utilization of full field sensors like cameras and microphones enables to delegate this to mathematical processes and surprisingly good monitoring results can be achieved which are far beyond human perceivability. Teaming of humans and machines needs a re-definition of roles and also modifications in the communication concept. The utilization of artificial intelligence (AI) in the entire concept requires the exploitation of different AI tools, namely tools which are adapted to the respective task to be solved. As machines are becoming experts in their manufacturing process by gaining information from skilled operators due to the self-learning and cognitive expert system ethic discussions become necessary. An example of thermal compensation of machines shows the performance gain with the AI application. In addition the benefit of fleet learning is demonstrated for this application.

REFERENCES: [1]Wegener K, Spierings AB, Teti R, Caggiano A, Knüttel D, Staub A (2021). A conceptual vision for a bio-intelligent manufacturing cell for Selective Laser Melting. CIRP Journal of Manufacturing Science and Technology 34: 61–83.

Microstructure of HIPped SLM-Ti6Al4V

E. Brunner[1], J. Wuttig[1], T. Plüss[2], L. D'Antoni[2], CBT. Ly[2], M. de Wild[2]

[1]Sauber Technologies AG, Hinwil, CH, [2]University of Applied Sciences Northwestern Switzerland FHNW, Muttenz, CH

INTRODUCTION: In the Selective Laser Melting (SLM) process, a 3D-object is created layer-by-layer by melting of powder. Its microstructure depends on process parameters [1] and thermo-mechanical post-processes [2]. It is known that the microstructure, especially in the binary titanium alloy Ti6Al4V (3.7165), can be adjusted by hot isostatic pressing (HIP) [3].

METHODS: Ti6Al4V samples for analysis were produced on a MetalFAB-SLM system, see Fig. 1. After a standard stress-release annealing, the samples were hot-isostatic pressed and controlled cooled at various process parameters. Tensile tests were performed according to DIN EN ISO 6892-1. The separated part was used for microstructure examination and etched according to Fuss by Struers. SEM investigations were performed using a Hitachi TM3030Plus system.

Fig. 1: Tensile tests sample with integrated microsection specimen (red box).

RESULTS: Fig. 2 shows that the microstructure is influenced by the cooling rate. In general, the higher the cooling rate, the finer the microstructure and the lamellar thickness.
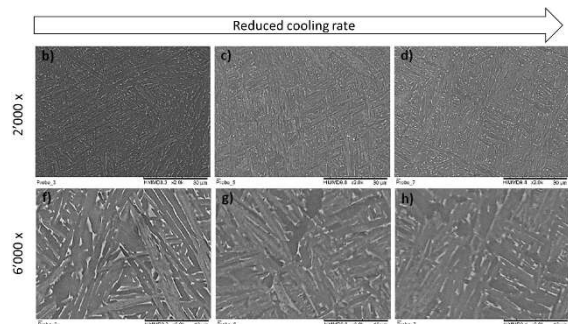
Fig. 2: Microstructure versus cooling rate. Top row magnification 2'000x (scale bar 30 µm), bottom row 6'000x (scale bar 10 µm).

Rapid cooling results in α lamellae and needle-like α'-phase. The α-martensitic phase within the β-phase is only visible after quenching. A higher annealing temperature leads to a coarser microstructure, see Fig. 3 top. As expected, elongation at break increases with decreasing cooling rate and coarser microstructure, while tensile strength and yield strength decrease, see Fig. 3 bottom.
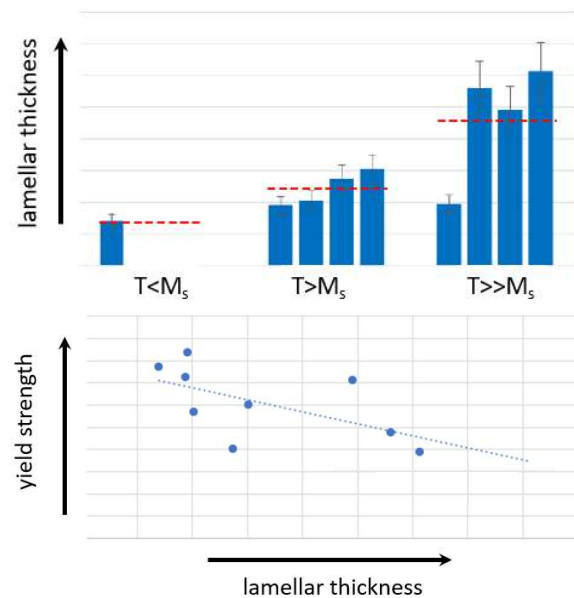
Fig. 3: Influence of hipping temperature on the microstructure (top) and relation between lamella thickness and yield strength (bottom).

DISCUSSION & CONCLUSIONS: It is shown that the microstructure and the mechanical properties of SLM-Ti6Al4V can be optimized to needs by HIP and controlled cooling.

ACKNOWLEDGEMENTS: We would like to thank Struers for etching the samples.

REFERENCES: [1]S. Liu et al., *Additive manufacturing of Ti6Al4V alloy: A review*, Materials & Design, 164, 107552, 2019. [2]A.D. Baghi, *Effective post processing of SLM fabricated Ti-6Al-4V alloy: Machining vs thermal treatment*, J Manuf Proc, 68, Part A, 1031-1046, 2021. [3]Y. Lu et al., *The Influence of heat treatment on the microstructure and properties of HIPped Ti-6Al-4V*, Acta Materialia, 165, 520-527, 2019.

Implants with complex open-pored cellular structure additively manufactured by LPBF using geometry adapted slicing functions

J. Thielsch[1], F. Gebhardt[1], S. Holtzhausen[2], C. Ortmann[3], M. Liebelt[3]

[1]Department of Laser Powder Bed Fusion, Fraunhofer Institute for Machine Tools and Forming Technology, 01187 Dresden, DE, [2]Chair of Virtual Product Development, Technische Universität Dresden, 01062 Dresden, DE, [3]Mathys Orthopaedie GmbH, 07646 Moersdorf, DE

INTRODUCTION: The aim of the work was to improve the dimensional precision of Laser Powder Bed Fusion (LPBF) parts by using suitable exposure strategies and machining parameters. Furthermore, the possibility to avoid costly and time-consuming coating steps for preparation of a complex open-pored cellular structure was investigated for potential implants.

METHODS: The manufacturing of test specimens and implant demonstrator parts was carried out by LPBF. The generation of the cellular structures is based on 3D voxel data. Defined voids are calculated, optimized according to size and subtracted from an envelope geometry. Afterwards, the geometry is analyzed with regard to adapted scan strategies for controlled fabrication of regular and irregular cavities. Preliminary, intermediate and final cleaning was carried out in various cleaning baths with washing solutions including the use of ultrasound and rotation. Compression tests were performed.

RESULTS: Areas with specific topographic features, as e.g. bridges, bulk or open-pored cellular features were automatically identified within the geometric model and assigned with adapted scanning strategies and laser parameters, respectively, using special slicing functions (see Fig.1 and Table 1).
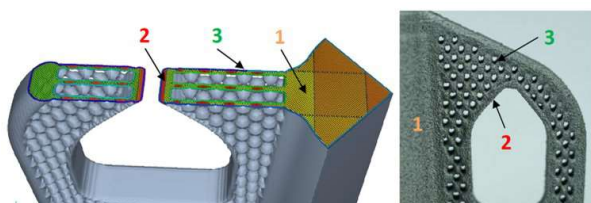
Fig. 1: Cross-section of a shoulder short shaft implant geometry (left) LBPF manufactured shoulder short shaft (right); marked regions are assigned with different LPBF parameters (see Table 1).

Table 1. LPBF parameters for different marked regions in Fig. 1.

Parameter	Laser power / W	Scan speed / mms⁻¹	Laser spot size / μm
1	105	600	100
2	112	700	100
3	100	625	100

A Young's modulus of 4.74 GPa is within the range of comparable osteo implants. Besides it was possible to clean the manufactured components successfully.

DISCUSSION & CONCLUSIONS: This new manufacturing approach resulted in higher dimensional accuracy as well as higher quality of the components (see Fig. 2).

LPBF - IWU   LPBF (OEM)
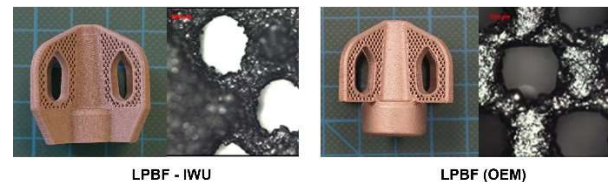
Fig. 2: Fabricated shoulder short shafts based on identical cellular geometry models and corresponding microscope images of cellular structure; LBPF manufactured at Fraunhofer IWU with adapted scan strategies (left) LPBF manufactured at OEM (right).

LPBF fabricated implants with cellular structures offer the potential to support osseointegration without external coatings. Investigations regarding biocompatibility without coating are still pending. In the positive case the production time would be reduced by 6 weeks and the production costs by 33 % compared to the conventional CNC-production route with additional coating step.

Additive manufacturing of zirconia canine resurfacing elbow joint prosthesis via digital light processing

D. Komissarenko[1], T. Graule[1], I. Burda[2], B. Weisse[2], S. Roland[3], B. Seeber[3], D. Koch[4], G. Blugan[1]

[1]Laboratory for High Performance Ceramics, Empa, Dübendorf, CH, [2]Laboratory for Mechanical Systems Engineering, Empa, Dübendorf, CH, [3]Metoxit AG, Thayngen, CH, [4]Kleintierchirurgie AG, Diessenhofen, CH

INTRODUCTION: Elbow dysplasia in dogs is a painful chronic, and potentially degenerative disease that is known to affect certain breeds of dogs, especially larger ones like Labradors, German Shepherds or Rottweilers. The present work aims to develop a ceramic resurfacing implant for dog elbows made by additive manufacturing for less invasive surgery. Digital light processing (DLP) was chosen as an additive manufacturing method to 3D-print the ceramic prosthesis, since it allows to produce the parts with unique design, very high spatial resolution and fine surface finishing. The method is based on the layer-by-layer solidification of a liquid photosensitive resin filled with ceramic powder *via* UV-light exposure followed by debinding of organic components and sintering.

METHODS: The photosensitive ceramic slurries were prepared via incremental addition of the zirconia or alumina powders into a mixture of acrylates and dispersants followed by a planetary ball milling. The solid content of the zirconia and alumina slurries was 35 vol.% and 40 vol.%, respectively. The implants and discs for mechanical testing were 3D-printed using Asiga Pico 2 (Asiga, Australia) and CeraFab 7500 (Lithoz, Austria) printers at different energy doses. The parts were manufactured with the thickness of the layers of 25 microns. The binder system from the parts was removed via thermal treatment at low heating rates. The sintering of the green bodies into dense ceramics was performed in air at 1480 °C for 2 h. The sintered ceramics was characterized via density measurement, SEM, XRD and ball-on-three-balls flexural strength tests.

RESULTS: The present study demonstrates the possibility of 3D-printing high quality zirconia ceramics with relatively low solid content in the slurry via development of a proper formulation, optimization of 3D-printing parameters and design of the debinding and sintering programs. The model of the implant and 3D-printed ceramic implants are presented in Fig. 1.
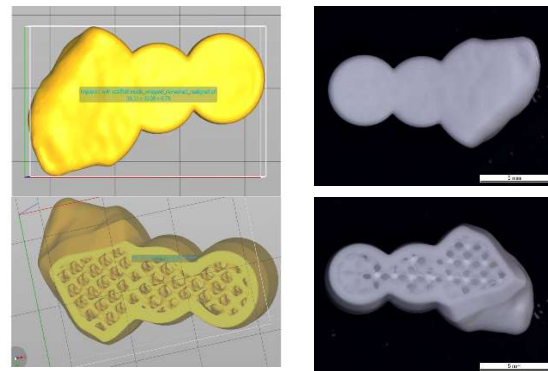
Fig. 1: The model of the implant with scaffold (left), the 3D-printed and sintered ceramics (right).

The density of both zirconia and alumina implants was close to the theoretical one. According to the ball-on-three-balls analysis the average strength of zirconia ceramics was 1566 MPa. The average grains size was 0.5 microns, according to the SEM.

DISCUSSION & CONCLUSIONS: Using 3D-printing, it was possible to manufacture high strength zirconia parts. Different designs of ceramic implants were evaluated for printability. A hydroxyapatite layer was added onto a scaffold part of the implant. Finally, the implantability of the designed implant prototypes was verified using cadavers of dogs.

Wireless Power Transfer for "Smart" Implants

S. Bauer, W. Döll, D. Ulrich

Helbling Technik Bern AG, Liebefeld-Bern, CH

INTRODUCTION: Several technologies for wireless power transfer are already available to developers of medical devices. The spectrum of electromagnetic solutions ranges from the low-frequency kHz to the high-frequency GHz range. On an example of an eye implant, we show which technologies for wireless power transfer are available today and how the most suitable one can be chosen.

METHODS: For the development of the wireless power transfer solution, we used simulation methods as well as testing in the high-frequency laboratory. For the simulation, a combination of self-developed and commercial simulation tools came into use to precisely represent the electromagnetic boundary conditions, including absorption in the surrounding tissue.

RESULTS: We developed a wireless power link for an electronic eye implant for continuous measurement of the intraocular pressure. Simulations showed that two variants were possible: a conventional solution in the near field using magnetic coupling at 13.56 MHz, and a solution in the far field at 900 MHz.
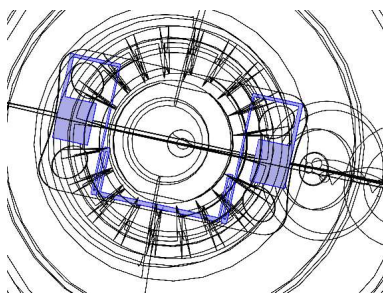
Fig. 1: Intra-ocular lens with antenna (in blue), simulation model of an anatomical eye.
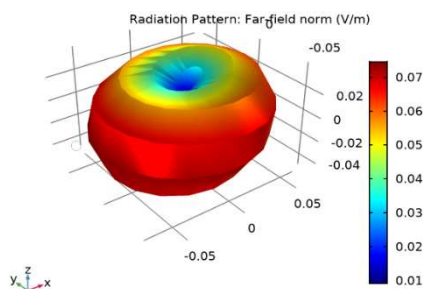
Fig. 2: Radiation characteristics of the Ultra High-Frequency antenna (simulation result).

A pre-clinical study with implants operating in the near field at 13.56 MHz was successfully completed and in-vitro testing confirmed the simulation results, which indicated a range of up to 1 m for wireless power transfer at 900 MHz. But there was another argument in favor of the latter solution: Because of the dielectric properties of the surrounding tissue, a UHF antenna at 900 MHz can be implemented with significantly smaller dimensions than an antenna in air. With proper design methods, it was even possible to place the antenna on the non-optical surface of an intraocular lens.

DISCUSSION & CONCLUSIONS: Over the past few years, we have developed various wireless power and data links for medical applications that work in the frequency range from 10 kHz to 2.5 GHz. Depending on the area of application, standard technologies such as NFC (13.56 MHz) or Bluetooth (2.4 GHz) can be employed. However, if the application-specific needs cannot be met with standard technologies, proprietary developments are used to close this gap.

In orthopaedics and other surgical fields wireless power transfer to implants might become more and more important. "Smart" implants such as the Zimmer Persona IQ© equipped with sensing and wireless data communication capabilities might need external power charging, as new functionalities will be added. Smart implants will have the potential to support the shift towards a more predictive, data driven health care approach.

REFERENCES: Khan, S.R.; Pavuluri, S.K.; Cummins, G.; Desmulliez, M.P.Y. Wireless Power Transfer Techniques for Implantable Medical Devices: A Review. Sensors 2020, 20, 3487.

H.-J. Kim, H. Hirayama, S. Kim, K. J. Han, R. Zhang and J. -W. Choi. Review of Near-Field Wireless Power and Communication for Biomedical Applications. In IEEE Access, vol. 5, pp. 21264-21285, 2017.

Surface treatments of 3D printed Nitinol stents

L. Jerjen[1], B. Schnyder[1], T. Journot[2], O. Banakh[2], J. Pralong[1], S. Rey-Mermet[1]

[1]*School of Engineering, HES-SO Valais, Sion, CH,* [2]*HE-Arc, Neuchâtel, CH*

INTRODUCTION: Above its austenitic/ martensitic transition temperature (TT), Nitinol is superelastic and below it has shape memory capacity. If TT is below the body temperature, the stent can be cooled and deformed to reduce its diameter before being inserted in the arteria. It will then recover its expanded geometry. Stents are currently produced by laser cutting or welding of Nitinol tubes or wires. In this work, stents are 3D printed by Selective Laser Melting (SLM).

METHODS: Stents have been printed by SLM with an SLM Solutions 125 printer by using an atomized Nitinol powder with a Dv50 of 35 μm and a composition of 50.8 at% of nickel. Printing parameters have been varied to adapt A_F that was measured by Differential Scanning Calorimetry on lattice structures. The minimal "wire" diameter obtained as printed was of 200 μm.

The stent surface has been treated by electropolishing (EP) to reduce its roughness. Two stainless steel 3D printed meshes, having the same patterns as the Nitinol stents have been used as outer and inner counter-electrodes. A parametric study has been performed to establish EP conditions: electrolyte molar ratios of KCl:ethylene glycol between 1 to 5 %, temperature of 80 °C or 130 °C with an applied voltage of 60 V.

After polishing, some stents have been coated by a 50 nm thick TiO_2 layer by Atomic Layer Deposition or by a 1 μm thick Tantalum layer sputtered by Physical Vapour Deposition.

Cytotoxicity in L929 cell cultures and hemocompatibility by osmotic fragility assay have been performed on as-printed, polished and coated stents according to ISO 10993-12 guidelines.

RESULTS: By varying the energy density between 73 and 250 J/mm³ and power from 50 to 250 W, it has been possible to control A_F between 27 °C and 98 °C in the stents. The stents have a wire diameter of approximately 200 μm before EP.

EP helps to reduce surface roughness to 13 nm (ISO 21920) on flat samples. For 3D structures polishing, stainless steel inner and outer counter electrodes have been printed by SLM. It has permitted to reduce the roughness significantly on the outside and the inside of the stents as shown on figure 1.
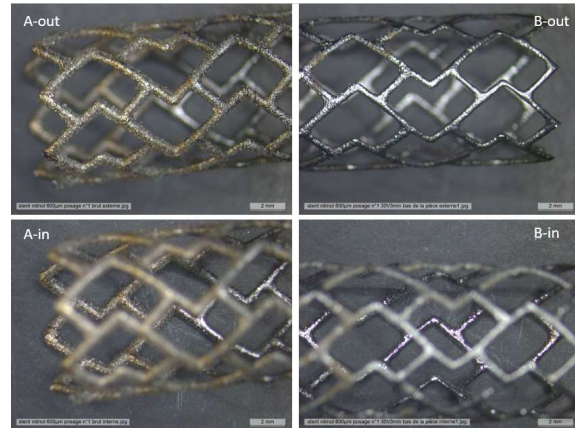
Fig. 1: A-out and A-in: outside and inside view of the mesh roughness as printed. B-out and B-in same views after EP

A mechanical deformation corresponding to a diameter contraction by a factor 4 has been successfully recovered by heating the stent up to 35 °C in hot water. Fatigue tests in radial compression have been realized on a specifically constructed setup. Stents survive at least 10^5 cycles with a radial deformation of 1%.

Cytotoxicity test have shown that all the 3 samples are bio- and hemocompatible. However, TiO_2 coating seems to significantly reduce the loss of red blood cells.

DISCUSSION & CONCLUSIONS: Stents with adequate mechanical and physical properties have been successfully printed by adapting SLM parameters and electropolished to reduce their inner and outer roughness. SLM has the advantage of reducing the number of processing steps and of allowing more geometry freedom. As printed, polished and TiO_2 coated stents are biocompatible and hemocompatible.

Micro-arc anodized magnesium AZ31 alloy: towards application in veterinary implants

O. Banakh[1], T. Journot[1], Y. Savary[1], A. Hämmerli[2], J.-C. Puippe[3]

[1]Haute Ecole Arc Ingénierie (HE-Arc), La Chaux-de-Fonds, CH,
[2]Kyon AG, Zurich, CH, [3]Steiger Galvanotechnique SA, Châtel-St.-Denis, CH

INTRODUCTION: Mg-based alloys can be used as biodegradable materials in cardiovascular and orthopedic implants. The aim of this study was to evaluate the AZ31 alloy for its use in veterinary implants. As the alloy is very sensitive to corrosion in biological medium, Plasma Electrolytic Oxidation (PEO) surface treatment has been applied to the implant to provide its mechanical integrity in the body over several months by slowing down the corrosion process.

METHODS: AZ31 implants (25 mm diam.) were produced by machining according to the design in Fig. 1 and post-finished by vibro-abrasion. PEO surface treatment was performed using a CIRTEM® bipolar pulsed current source (f=500 Hz; J+= 24÷64 A/dm^2). The electrolyte used was a mixture of 2.8 g/l NaOH and 7.5 ml/l Na_2SiO_3 (pH=12.5). Treatment time was 5 min. The surface and cross-section morphology of the treated samples were examined by Scanning Electron Microscopy (SEM) and optical microscopy. Corrosion degradation tests were performed by immersing the samples in a simulated body fluid (SBF, Ringer solution) at 37 °C during 40 days. For some samples, hydrogen gas release was also measured. Mechanical tests were performed on the PEO-treated implants before and after several weeks of immersion in a SBF solution. The test consisted of applying a progressive force perpendicular to the surface of the implant. During the test, the applied force and the displacement of the implant were recorded.

RESULTS: The current density used in PEO process shows an influence on the surface morphology of the anodized layer. The PEO layer exhibits the pores ranging from 5 to 10 μm in diameter as well as the cracks, usually obtained by this process. The layer is homogeneous in thickness over the entire implant geometry. Metallographic tests showed an anodized layer thickness of about 10-15 μm. The chemical EDX analysis showed mainly Mg and O peaks confirming the presence of oxidized magnesium. The influence of current density on the corrosion resistance of the implants is less significant. Potentiodynamic tests showed a decrease in the corrosion current of PEO-treated parts by a factor of 700 as compared to untreated AZ31 samples.

The mechanical strength of PEO-treated implants is satisfactory. The coating slightly affects the mechanical strength of the implant, decreasing the force required to bend the implant 2 mm by 40 N. The mechanical strength of the implant decreases as the implant degrades. After 5 weeks immersed in SBF, the force required to bend the implant 2 mm dropped from 700 N to 600 N (Fig. 2).
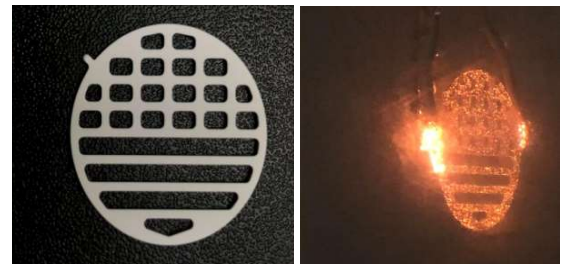
Fig. 1: The prototype implants: before (left) and during PEO treatment (right).

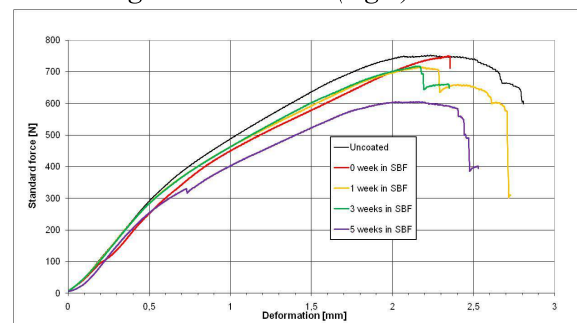*Fig. 2: Mechanical tests performed on the untreated (black curve) and PEO treated implants after their immersion into SBF solution up to 5 weeks.*

DISCUSSION & CONCLUSIONS: PEO treatment has significantly improved the corrosion resistance of AZ31. Mechanical tests showed good mechanical stability of the treated implants after their immersion in SBF for 5 weeks.

Anti-bacterial coating for implant surfaces based on electrochemically-formed calcium hydroxide

H. Holeczek[1], O. Braissant[2], J. Rüegg[3], M. de Wild[3]

[1]Medicoat AG, Mägenwil, CH, [2]University of Basel, Allschwil, CH, [3]University of Applied Sciences and Arts Northwestern Switzerland, Muttenz, CH

INTRODUCTION: Increasing numbers of cases with infection after implant operation drive the demand for an anti-bacterial property of the implant surface. Such a bactericidal effect should be strong enough to kill bacteria that might reach the implant surface during or after the surgical procedure. On the other hand, it should not affect the body of the patient with possible long-term effects.

METHODS: Titanium disks and screws have been coated with a rough titanium layer by thermal plasma spray coating first. Samples were then coated with a compound layer of $Ca(OH)_2$. The surface of the coated samples was then moistened with LB medium containing *S. epidermidis* and *S. aureus* with a concentration of 10^5 CFU ml^{-1}. Samples were then placed in a micro-calorimeter.

RESULTS: Activity of the bacteria was measured indirectly via the produced metabolic heat. The diagram resulting from Gompertz curve fitting (Fig. 1) shows the reduced metabolic heat for the $Ca(OH)_2$ coated sample.
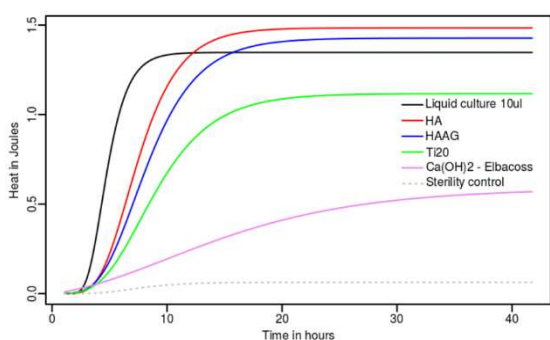
Figure 1: Modelled data from Gompertz curve fitting of micro-calorimeter measurements.

The growth rates of the different populations (Fig. 2) were calculated from the measurement data and show a considerably reduced growth on the samples with anti-bacterial $Ca(OH)_2$-coating, compared to those with hydroxyapatite (HA) or pure titanium (Ti20).
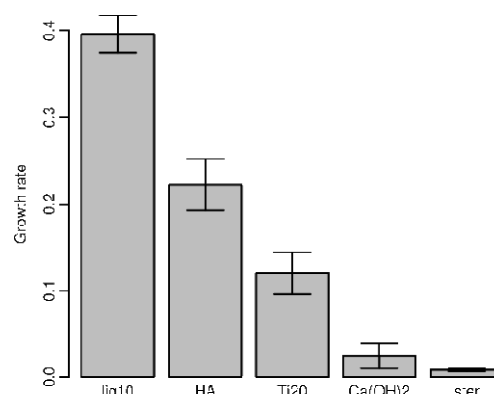
Figure 2: Growth rates computed from calorimeter data.

DISCUSSION & CONCLUSIONS: Measurements with a micro-calorimeter have been used to indirectly detect the bacterial metabolism activity by measuring the heat generated. On samples coated with $Ca(OH)_2$ a significant reduction of bacterial activity was detected which points to greatly reduced growth of the initial organisms. Thus, the anti-bacterial effect of such a coating has been shown.

As the coating consists only of Ca and hydroxyl ions, which are both completely resorbed by the body, the active coating is removed after some time. The contact-killing effect is only active directly on the surface of the coated specimen. Yet, there is no risk of long-term effects to be expected when the coating is used in the body. Furthermore, our in-vivo study showed good osseointegration of coated implants in rats [1].

REFERENCES:
[1]N. Harrasser, M. de Wild, J. Gorkotte, A. Obermaier, S. Feihl, M. Straub, R. von Eisenhart-Rothe, H. Gollwitzer, J. Rüegg, W. Moser, Ph. Gruner, R. Burgkart, *Evaluation of calcium dihydroxide- and silver-coated implants in the rat tibia*, J Appl Biomater Funct Mater 14(4): e441-e448 (2016).

Artificially induced peri-implant inflammation around mechanically loaded Zirconia and Titanium implants.

S. Wolf[1], CM. Sprecher[2], S. Milz[3], H. Woelfler[4], M. Gahlert[1], S. Janner[5], B. Meng[6], DL. Cochran[6], S. Roehling[1]

[1]University of Basel, CH, [2]AO Research Institute, Davos, CH, [3]University of Munich, DE, [4]University of Bamberg, DE, [5]University of Berne, CH, [6]University of Texas, USA

INTRODUCTION: The present study aims to investigate the influence of an implant material on the mineralized tissue response in artificially induced peri-implant inflammation and infection around the upper part of mechanically loaded dental implants.
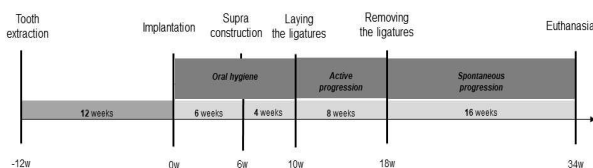
Fig. 1: Timeline illustrating the different phases of the study.

METHODS: Five male dogs (American Foxhound) received 4 implants (Titanium or Zirconia, randomly assigned position, micro-rough surface topography) on each side of the jaw. The implants were placed in preconditioned bone with the original teeth removed 12 weeks before implantation (Fig. 1). After installation of the load bearing supra construction, ligatures around the implant neck were installed to induce local inflammation. Eight weeks later ligatures were removed and 16 weeks later animals were euthanized and bone/implant blocks (including the gingiva layer) were obtained.
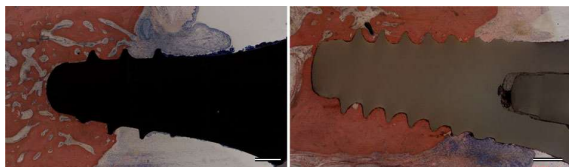
Fig. 2: Histological images of Titanium (left) and Zirconia (right) implant sections stained with Giemsa Eosin. Scale bars: 1000 μm.

After preparation of resin embedded Giemsa/Eosin-stained sections (Fig. 2), peri-implant bone density and peri-implant contact ratio and bone loss of the alveolar crest were histomorphometrically determined in a buco-lingual plane.

RESULTS: Bone resorption around Titanium implants was significantly increased compared to Zirconia implants. The effect was most pronounced on the lingual side (Fig. 3). Other parameters did not show significant differences. All implants clinically appeared to be stable.
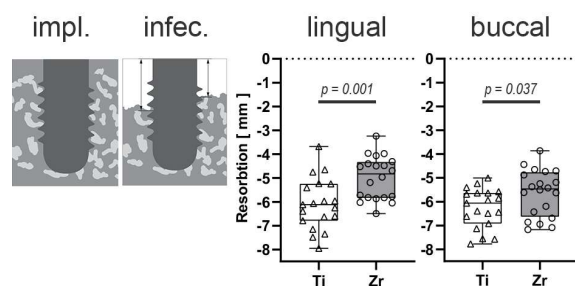
Fig. 3: Significantly increased bone resorption around Titanium implants compared to Zirconia implants, especially at the lingual side. The schematic illustrations show bone around the implant after implantation (impl.) and after continuous inflammation and accompanying infection (infec.).

DISCUSSION & CONCLUSIONS: Mechanically loaded Zirconia implants exhibited significantly reduced peri-implant bone loss at the end of a 16 week healing phase after artificially, ligature-induced inflammation, when compared to Titanium implants with a comparable surface topography and roughness. The histological results are in line with radiological results, already published in the literature [1].

REFERENCES:
[1]Stefan Roehling et al Int J Oral Maxillofac Implants 2019:357–365.

Clinical Applications of Patient-Specific Implants: How to Avoid Reinventing the Wheel

H. Yau[1], EWF. Yau[1], C. Fang[2,3], CHB. Yung[1]

[1]KOLN3D Technology SA, Geneva, CH, [2]The University of Hong Kong

INTRODUCTION: Patient-Specific Implants (PSI) have been demonstrated to have potential in significantly improving patient outcomes and post-operative quality of life. However, there are unavoidable risks associated with the use of a bespoke product during a surgical procedure that often strays from standard procedure and requires specific attention. Hence it is imperative that the scope of application regarding patient-specific implants be flexibly determined on a case-by-case basis to mitigate unnecessary risk exposure [1], [2].

METHODS: Patient-specific implants were planned, designed, fabricated, tested, and surgically implanted by a surgeon-lead collaborative team between the University of Hong Kong and KOLN3D Technology. Extent of implant customization was adapted for case specifics and needs. Cases were and will be followed up for up to a year post-op to evaluate efficacy of PSI.

RESULTS: Three case studies will be shared as examples of varying extents of application by patient specific implants within the greater surgical context. The first case is that of a hip replacement resulting from a tumor resection that utilizes a patient-specific hip reconstruction that is affixed to a commercial acetabulum cup/femoral stem (Fig. 1). The second case is a temporomandibular joint replacement employing a patient-specific mandible component and a commercial UHMWPE temporal bone component.
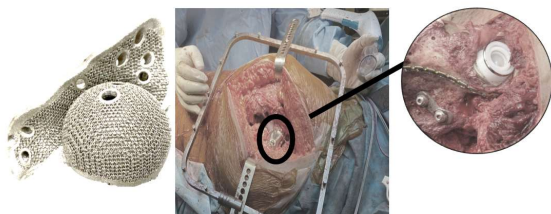
Fig. 1: Hip Reconstruction PSI with commercial acetabulum cup and femoral stem.

The third case is a talar replacement completely bespoke (Fig. 2), with osteoinductive features to promote improved biological integration.
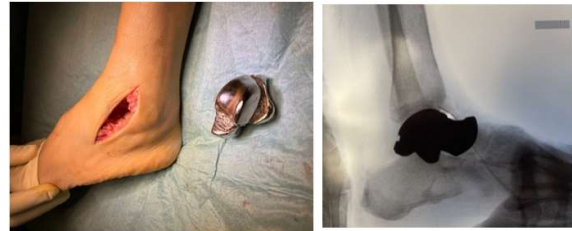
Fig. 2: Bespoke Talar Replacement Implant.

DISCUSSION & CONCLUSIONS: All surgeries were completed without complication. No surgical revisions associated with implant failure were required.
By identifying benefits of patient-specific implants and utilizing standardized products where possible, Health and Quality of Life improvements to the patient are maximized whilst risk exposure is controlled.

REFERENCES: [1]Y.N. Chim, S.K.H. Chow, S.Y. Mak, M.M.C. Li, B.C.H. Yung, E.W.F. Yau, C.S. CHUI. (2020) 3D-printed cobalt-chromium porous metal implants showed enhanced bone-implant interface and bone in-growth in a rabbit epiphyseal bone defect model. Bone Reports. 13. 100375. 10.1016/j.bonr.2020.100375.
[2]C. Fang, H. Cai, E. Kuong, C.S. CHUI, Y.Y.C. Siu, T. Ji, I. Drstvensek (2019) Surgical applications of three-dimensional printing in the pelvis and acetabulum: from models and tools to implants. Der Unfallchirurg. 122. 10.1007/s00113-019-0626-8.

Challenges and *in-vitro* solutions for the biocompatibility assessment with chemical characterization based on ISO 10993

S. Savic, S. Weissensteiner, D. Neubert, E. Mertl

OFI – Austrian Research Institute for Chemistry and Technology, Vienna, AT

INTRODUCTION: The biocompatibility assessment of medical devices is regulated in the MDR, not specifying how this information shall be retrieved. The ISO 10993 series is therefore THE regulative tool routinely applied for the biocompatibility assessment of medical devices. By categorizing products by contact (blood, mucosa, intact skin) or duration, different endpoints or hazards need to be tested. The hazards addressed in ISO 10993 can be assessed step by step. However, considering the list for a hip implant, eleven endpoints would need to be evaluated. This can quickly become a very expensive task. Alternatively, a chemical characterization is the first step. Substances that are found in the system can further be identified and risk assessed based on substance information and amount.

For the extraction, the ISO serves as guideline and sets extraction conditions, however, here some problems may occur. As the solvents tend to overestimate the conditions present in the human body and are way too harsh, samples are often damaged. Here the question arises in how far the chosen conditions reflect the true nature of the application.

If during the identification unknown substances remain, these knowledge gaps can be overcome by using alternative *in-vitro* methods.

METHODS:

Chemical Characterization: Due to chemical differences (polarity, organic/ inorganic; metals, etc.) a complete characterization requires three different methods. These are the HPLC-MS system, a GC-MS system and the ICP.

In – vitro tests: Cytotoxicity is determined using L929 Cells and exposing a samples' extract in cell culture medium for 24 h to the cells. Sensitization is done with an MDA-ARE cell line, that upon the exposure of potentially sensitizing substances activates the ARE-Nrf2 pathway that later can be visualized. The second test for sensitizing potential is the *in-chemico* DPRA assay, where the potency of a sample extract to bind to amino acids Lysine and Cysteine is estimated. The test for irritation is based on human skin models where extracts are exposed to for 18 h.

RESULTS: In case no complete characterization of the detected substances is possible, the various *in-vitro* and *in-chemico* assays can provide suitable additive information of the different hazards. For the case that everything is well characterized but no literature on these substances can be found, the tests are also serving their necessity as certain hazards can be excluded.

The second problem is depicted in Figure 1 showing an experimental extraction of samples with different solvents. The advantage is that weaker solvents mimic the human body more realistically and are compatible with skin models or cell cultures whilst not damaging the sample. On the other hand, for hazard identification worst-case solvents are required.

Fig. 1: Effect of different solvents on the same sample in plane and moulded form.

DISCUSSION & CONCLUSIONS: In a case study all substances identified could be risk assessed, resulting in no need for further *in-vitro* tests. For the case that a sample is obviously damaged the extraction conditions can be altered and solvents diluted to prevent damage, but no complete shift will be possible. Animal free alternative tests are a great additional tool to on one hand complete the picture and on the other use solvents that reflect more realistic conditions. Nevertheless, the problem of extracting unrealistically too much by exaggerated conditions remains an issue of argumentation in the report.

In vitro testing of degradable magnesium implants – Avoiding the pitfalls

H. Schmotzer[1] and S. Rogge[2]

[1]SigmaRC GmbH, Cham, CH, [2]botiss biomaterials GmbH, Berlin, DE

INTRODUCTION: Biodegradable magnesium (Mg) implants have been introduced in orthopaedic and vascular surgery over the last decade. Most recently, implants for oral regenerative applications have been added. Mg and its alloys combine good mechanical properties, excellent biocompatibility, and the ability to degrade in a reasonable time period.

Extensive preclinical testing is required for regulatory submission. Commonly, test strategies follow established pathways based on pertinent standards and regulations, which have been developed and validated using inert devices. Testing laboratories obtain accreditation tests built on these standards.

In vitro testing of biodegradable Mg using established methods presents an extra challenge as the break-down is by corrosion which is a chemical reaction between the implant and its surrounding. Hydrogen development during degradation is a well-known phenomenon.

In the following, examples are provided, how this may lead to false-negative results when established protocols are used.

Example 1: Magnesium based products may come into contact with various substances during manufacturing. Here, a nitric acid containing solution was used for surface finish. After extraction of the finished device the residual contamination by nitrates (NO_3^-) was below the detection limit. After packaging and accelerated aging @ 60 °C black stains occurred. Samples were sent for ToF-SIMS analysis comparing stained and unstained regions. Dark zones showed only a mild signal intensity for nitrates; however, a strong signal was measured for nitrites (NO_2^-) suggesting that the nitrates had been reduced by the Mg. XPS analysis of such regions demonstrated a complete absence of metallic Mg. All Mg was in the oxidised state. In contrast, unstained regions showed approximately 20% metallic Mg.

Example 2: During final cleaning, medical devices are commonly rinsed in EtOH or IPA to replace the water and accelerate drying.

Mg is rather soft and may easily be scratched even when using polymeric tools. Metallic Mg sheets were mildly scratched and suspended in EtOH. After drying, packaging and accelerated aging @ 60 °C the scratches turned dark grey to black. ToF-SIMS analysis demonstrated oxidised Mg in the dark markings as well as short, oxygenated hydrocarbons suggesting the formation of ethanolates in the scratches which were reduced during ageing.

Example 3: Particle burden on medical devices is determined as part of the validation of the cleaning process (ISO 19227, ASTM F3127). Commonly, particles are determined using the water-based extracts for TOC (ASTM F2459). However, depending on the type of alloy and surface treatment, corrosive processes during extraction may start to release particulates. Device testing resulted in a residual particle burden of 77.7±8.3 µg/sample which would have been well above the specific acceptance level. After rinsing the filters with 5% nitric acid, the particle burden was below the detection limit of 17 µg/sample.

Example 4: Similarly, suspended corrosion products may influence pH and osmolarity of extracts when conducting cytotoxicity testing according to ISO 10993-5 if unfiltered or uncentrifuged extracts are used. The individual corrosion rate of a given alloy influences Mg concentration, pH and osmolarity as demonstrated by Fischer et al. [1].

DISCUSSION & CONCLUSIONS: Mg is highly reactive directly affecting its immediate environment unlike other already established biodegradable materials which generally break down by dissolution or hydrolysis. This needs to be assessed during the creation of a test plan for preclinical studies prior to actually starting them. Controlled and documented deviations from the standard laboratory procedures may be necessary to avoid undue rejection of a material or device.

REFERENCES: [1]Fischer et al. (2011) Improved cytotoxicity testing of magnesium materials. Materials Science and Engineering: B; Volume 176, Issue 11, 830-834.

Poster Session

1	*Supercritical CO$_2$ machining of titanium - a potential game changer* Erik Poulsen, GF Machining Solutions, Biel, Switzerland
2	*Direct Part Laser Marking in the Medtech Industry – How to make UDI-Code Marking safe and compliant* Christian Söhner, FOBA Laser Marking + Engraving | ALLTEC Angewandte Laserlicht Technologie GmbH, Selmsdorf, Germany
3	*In-silico comparison of topology-optimized acromion Levy type II implants* Janick Zehnder, FHNW, Muttenz, Switzerland
4	*Duplex technology to improve osteointegration of PEEK implants* Sophie Farine, Haute Ecole Arc, La Chaux-de-Fonds, Switzerland
5	*Comparative study of particle loads in peri-implant soft tissue over osteosynthesis plates made of CFR-PEEK and titanium* Christoph Sprecher, AO Research Institute, Davos, Switzerland
6	*In-silico implant validation: Establishing a reliable computational bone-implant model* Michaela Maintz, FHNW, Muttenz, Switzerland
7	*In-vitro validation of operational strength of impact-loaded surgical instruments by means of an automated pendulum impact tester* Matthias Brensing, IMA Materialforschung und Anwendungstechnik GmbH, Dresden, Germany

Supercritical CO_2 machining of Titanium; a potential game changer

E. Poulsen[1], B. Azarhoushang[2]

[1]GF Machining Solutions, Biel, CH, [2]Institute of Precision Machining (KSF), Furtwangen University, Tuttlingen, DE

INTRODUCTION: The effects of supercritical CO_2 cooling (Sc-CO_2) on the high-speed milling of titanium grade 5 (Ti6Al4V) using a Mikron MILL S 400 U® 5-axis milling machine, equipped with a StepTec 42k spindle, and a Fusion Coolant Systems Pure-Cut+® Sc-CO_2 delivery system was studied at various cutting parameters and compared with flood coolant milling using emulsion. The effects on tool wear, achievable MRR, surface roughness and micro-hardness were evaluated.

METHODS: The experiments were divided into five steps each with different cutting parameters where cutting speed (Vc) was varied from 110 to 200 m/min. A new tool was used continuously for each Sc-CO_2+MQL (minimum quantity lubrication; 2 ml/min of medical grade oil) and emulsion from step 1 up to step 4. The main aim was to analyse the achievable material removal rate for both coolant systems. At step 5 a high volume of material (113,850 mm^3) was machined using new tools (for both Sc-CO_2+MQL and emulsion) to assess the tool life and machining performance in detail.

RESULTS: At the end of each test step, the tool wear progression was monitored; no significant differences could be detected up to the step 4 of the tests. However, after Step 4, the cutting edges and rake faces of the tools show significant differences. The emulsion tool was severely damaged. In contrast, the CO_2 tool edges are not damaged as severely and the tool can still continue cutting.
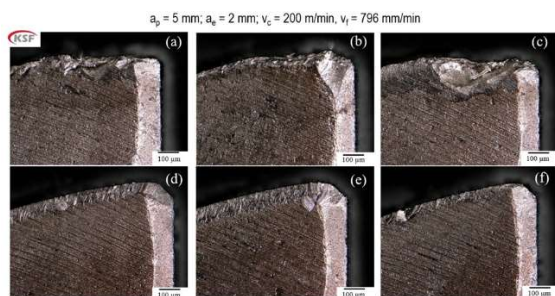

Fig. 1: Tool wear (rake faces) under traditional flood coolant (top 3 images a -c) and using sc-CO_2 (lower 3 images, d-f).

The represented differences between the cutting forces (Fy) of the emulsion tool and Sc-CO_2 tool were analysed during step 5 of the machining process and confirms the higher performance of sc-CO_2. Indeed, the cutting forces induced by the Sc-CO_2 tool are constant during the long time material removal and much lower than the emulsion tool in all performed machining passes, becoming much more prominent (up to 65% lower) when the 45th pass of the machining process was accomplished, indicating much higher tool wear rate for the emulsion tool.
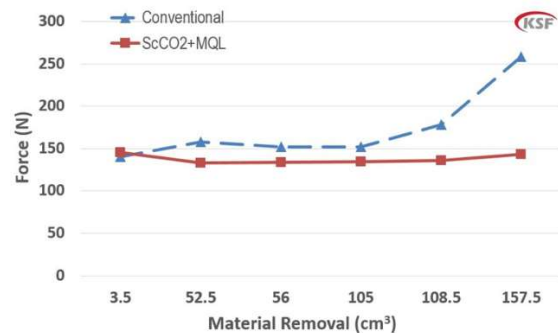
Fig. 2: Cutting Force vs. Material Removal

Additional measurements were taken comparing burr formation, surface roughness and surface micro-hardness - all showed benefits to the use of sc-CO_2 as a coolant.

DISCUSSION & CONCLUSIONS: The results of the tests conducted showed that, as compared to flood coolant milling, the use of Sc-CO_2 milling led to:

- reliable machining at significantly higher Material Removal Rates (MRR)
- significantly increased tool life (up to over 100 %)
- significantly lower cutting forces (up to 50 %)
- increased surface micro-hardness (up to 30 %)
- reduced surface roughness (up to 50 %)

We believe this technology has the potential to improve machining efficiency, reduce the pollution and energy consumption (through reduction or elimination of washing to remove emulsion), improve mechanical properties of the machined material, and reduce the risk to patients (through the reduced risk of contamination from residual cutting fluids).

Direct Part Laser Marking in the Medtech Industry
– How to make UDI-Code Marking Safe and Compliant

C. Söhner

FOBA Laser Marking + Engraving | ALLTEC Angewandte Laserlicht Technologie GmbH, Selmsdorf, DE

INTRODUCTION: Manufacturers of medical instruments or implants are currently challenged with increasing requirements regarding the UDI (Unique Device Identification) of their products. Each product has to be centrally registered and officially certified, but it also needs to bear an individual UDI-code which makes each product traceable throughout its entire life cycle.

METHODS: A UDI-code consists of a human and a machine-readable part in form and content, so that it matches the requirements of the FDA and the MDR. A UDI also needs to be applied directly on the surface of a medical product, it is used and processed multiple times.

To fulfil these requirements, manufacturers need to integrate an appropriate marking procedure in their production process. A laser marking system can ensure the durability and legibility of a UDI-code which is necessary for product traceability.

What makes a laser marking process safe and compliant? FOBA offers an innovative three-step marking workflow which includes pre-mark validation of the product, automated mark alignment, even if the product is placed at a random position within the marking field, and a post-mark validation of quality, content and position of the markings.

The so called "Medical Plug-in" is a software which helps medical device manufacturers to implement a safe and secure UDI-marking process for its validation.

RESULTS: The main goal of the UDI system is to enhance patient safety by means of medical device traceability. In the case of product recalls, it is possible to track every single part from its manufacturing until the use on the patient.

Considering implants, a UDI also facilitates the registration into centralized implant databases e.g. EUDAMED or GUDID. This also results in better implant quality control. A UDI also helps to streamline part processing in manufacturing

or in the hospital cleaning and sterilization procedures.

Fig. 1: Medical clamp with laser marked UDI code: To improve the readability of the code and characters, the laser created a white background (frosting).

DISCUSSION & CONCLUSIONS: The process of finding the appropriate laser marking parameters for a specific material can be tedious and time consuming. In most cases these are trial and error processes. The goal is to share the knowledge of key parameters to create a safe and secure UDI marking process.

The FOBA application team has developed innovative solutions out of 12 independent variables such as laser source, the optic used and the desired final effect to create the best laser marking results. In this way the operator receives the optimum laser parameters for lasting and secure UDI laser marks.

REFERENCES: Case Study: RUDOLF Medical - Lasers as the standard of the future for the marking of surgical scissors and instruments (https://www.fobalaser.com/applications/case-studies/rudolf-medical/).

Medical Industry White Paper - Unique Device Identification (UDI) Requirements, deadlines, secure labelling according to FDA and MDR (https://www.fobalaser.com/applications/case-studies/udi-whitepaper/).

In-silico comparison of topology-optimized acromion Levy type II implants

J. Zehnder[1], D. Seiler[1], R. Baumann[2], K. Eid[3]

[1]*UAS Northwestern Switzerland, School of Life Sciences, Muttenz, CH, [2]Lucerne UAS, CC Mechanical Systems, Horw, CH, [3]KSB, Clinic for Orthopaedics & Traumatology, Baden, CH*

INTRODUCTION: Acromion Levy type II fractures following reverse shoulder arthroplasties (RSA) are an exemplary indication showing the complicated elaboration of suitable implant designs due to various superimposed loading scenarios. Literature shows that only few studies are available investigating the true cause of why such fractures occur. In addition, no specific implant designs exist to treat these fractures specifically. This project aims to explain, in form of a conceptual (qualitative) structure mechanical in-silico investigation, why acromion Levy type II fractures occur, how modern design tools can be used to develop suitable implants and how these perform compared to a lateral clavicle plate (LCP).

METHODS: A digital 3D cortical bone model, based on the CT data of an 83-years old female patient, was developed for a shoulder complex consisting of scapula and clavicle. Literature-reconstructed muscle force vectors of the anterior, middle and posterior deltoid muscle [1] were used to setup a patient-specific finite-element model describing the biomechanical behaviour for abduction and flexion in the range of 15° to 120°. Automated parametrization studies were performed to analyse angle-specific stresses and deformations in the Levy type II area. Sensitivity analyses were used to investigate the sensitivity of resulting parameters upon changes in the magnitude, orientation and origin of muscle force vectors. After the identification of critical loading scenarios, the setup for the development of topologically optimized implant designs was elaborated. With the help of current movement studies, all investigated abduction and flexion angles were weighted according to their frequency of occurrence throughout the day. Through an iterative approach, while continuously simplifying the model and varying optimization constraints, final implant designs were generated for a preventive (pre-Levy II fracture) and curative (post-Levy II fracture) treatment, following an RSA. The final implant designs were benchmarked against an LCP.

RESULTS & DISCUSSION: The simulation studies revealed locations of potentially critical equivalent stresses below the acromion arc and maximum principal stresses on the superior-anterior border on the acromion, which may promote the start of a Levy type II fracture. The sensitivity analyses showed that equivalent stresses below the acromion arc significantly increased for abduction and flexion if vectors are increasingly directed in inferior or anterior orientation. This increased the resulting bending and torsional moments in the Levy type II area. An anteriorization of the shoulder joint centre revealed the most significant equivalent stress increase below the acromion arc. The final benchmarking of topologically optimized implant solutions against an LCP revealed better performance, mainly convincing through an improved anatomical fit, a better mass exploitation and more homogeneous stress distributions (*Fig. 1*) may leading to an advantageous fatigue life behaviour.
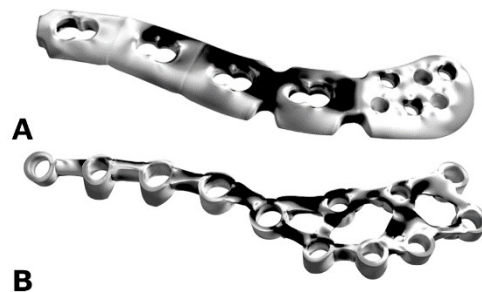
Fig. 1: Qualitative comparison of most critical (=black) equivalent stress distributions during post-operative abduction at 65° for a standard LCP (A) and a topology-optimized solution (B).

CONCLUSIONS: Finite-element analyses and topology optimizations are powerful tools for the analysis of complex biomechanics. Nevertheless, performing valuable topology optimizations in the field of biomechanics requires a detailed understanding of the method, as well as validated models to deliver usable outputs.

REFERENCES: [1]D. C. Ackland et al, J. Orthop. Res., 2011, vol. 29, no. 12, 1850–1858.

Duplex technology to improve osteointegration of PEEK implants

S. Farine-Brunner[1], O. Banakh[1], B-O. Aronsson[2]

[1]University of Applied Sciences of Western Switzerland (Haute Ecole Arc), La Chaux-de-Fonds, CH, [2] Nano Bridging Molecules SA, Gland, CH

INTRODUCTION: PEEK is widely used in medical fixation devices for orthopaedic, cranio-maxillary, spinal and trauma implants. The main advantage of PEEK is its Young's modulus, close to that of a human bone. Moreover, PEEK is extremely strong, durable, highly resistant to creep and fatigue, it withstands sterilization, and is radiolucent. The only disadvantage of PEEK is that it is a bioinert material with a highly hydrophobic surface, resulting in poor cytocompatibility and insufficient osteointegration.

The aim of this study is to develop a surface treatment to improve osteointegration of PEEK implants. In partnership with the company Nano Bridging Molecules SA (NBM), an innovative duplex surface treatment was developed combining Atomic Layer Deposition (ALD) technology and multi-phosphonate functionalization by dip coating (commercialised as SurfLink™ by NBM). Multi-phosphonates are used to improve osseointegration and long-term success of dental implants [1]. The proposed method showed promising results, a hydrophilic surface with a conformal coverage and increased cytocompatibility with osteoblast cells.

METHODS: First, a titanium dioxide layer is deposited by ALD on PEEK, followed by a multi-phosphonate layer (SurfLink™, NBM) deposited by dip coating. The SurfLink™ coating is known to improve the osteointegration of titanium surfaces. Cell inseminations are done on 3D printed (A) bare PEEK and the same PEEK coated with (B) TiO_2-ALD and (C) TiO_2-ALD-SurfLink™. Two different osteoblastic lines were used, SaOS and HOS, over a period of 2 weeks. Three independent experiments in triplicate were performed.

RESULTS: It was noticed that a minimum TiO_2-ALD layer thickness of 50 nm is crucial for achieving a high coverage of the multi-phosphonate coating (SurfLink™).

After 10 days of seeding, an increase by a factor of 1.2-1.4 in cell proliferation was observed on the coated PEEK samples as compared to a bare PEEK (Fig. 1).
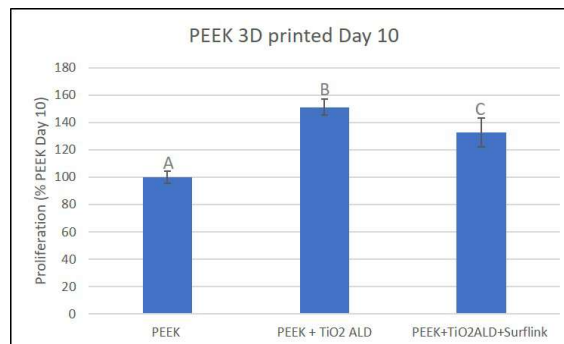

Fig. 1: Proliferation rate of osteoblasts 10 days after seeding on a bare 3D printed PEEK, coated with TiO_2-ALD and TiO_2-ALD-Surflink. Data expressed in % (100% is for bare PEEK) at day 10.

DISCUSSION & CONCLUSIONS: In our study, osteoblast (SaOS and HOS) proliferation on treated PEEK is significantly better for both treatments, TiO_2-ALD and TiO_2-ALD-Surflink vs. untreated PEEK. The results are slightly better for TiO_2-ALD as compared to TiO_2-ALD-SurfLink™. These are very first results and must be further confirmed, however it can be supposed that both treatments are fully suitable to enhance osteoblast proliferation on PEEK substrate. According to the studies carried out by NBM [1], SurfLink™ layer on titanium leads to an increase in early and mainly for long-term osseointegration as compared to untreated titanium.

Other tests according to ISO 10993 should be carried out to implement this surface treatment on industrially produced PEEK implants.

REFERENCES:
[1]http://www.nbmolecules.com/documents/superior-surflink-characteristics.pdf

Comparative study of particle loads in peri-implant soft tissue over osteosynthesis plates made of CFR-PEEK and titanium

E. Fleischhacker[1], CM. Sprecher[2], S. Milz[3], R. Wirz[4], R. Zboray[5], A. Parrilli[5], MM. Saller[1], T. Helfen[1], W. Böcker[1], B. Ockert[1]

[1]*Musculoskeletal University Center Munich, DE,* [2]*AO Research Institute Davos, Davos, CH,* [3]*Anatomische Anstalt der Ludwig-Maximilians-Universität, München, DE,* [4]*RMS Foundation, Bettlach, CH,* [5]*EMPA, Dübendorf, CH*

INTRODUCTION: For locked plating of proximal humerus fractures, implants made of various materials are currently available. After titanium gradually replaced steel as the leading material in recent years, plates made of polymers such as carbon fiber reinforced polyetheretherketone (CRF-PEEK) became available. To the authors' knowledge, however, no publication has analysed the human tissue response to these novel materials for treatment of proximal humerus fractures.

METHODS: 16 patients (55.2±15.33 years; 62.5% female) with limited shoulder motion and/or persistent pain (n=8 titanium, Philos, DePuy Synthes; n=8 CFR-PEEK, PEEKPower humeral fracture plate, Arthrex) were examined. The peri-implant soft tissue, and plates were removed 13.7±5.8 months after fracture treatment. The soft tissue reaction and foreign bodies were identified and characterized using routine histology, immunohistochemistry, high-resolution computer tomography (CT), light, electron and infrared microscopy.

RESULTS: Histological sections from tissue adjacent to CFR-PEEK plates contained a large number of carbon fibers (Ø3 μm, Fig. 1) and round PEEK objects (Ø<5 μm).
Immunohistochemically, 6 samples were significantly positive for inflammation related markers (CD163, 25F9, CD68, MRP 8/14). In the tissue over titanium plates, a few scattered particles of titanium (Ø<3 μm) were identified, with slight CD68 reaction in 5 and low MRP8/14 reaction in 3 samples. PEEK and the carbon fibres were identified by infrared microscopy.
The surface of explanted CFR-PEEK plates showed exposed and broken carbon fibres (Fig. 2), whereas the titanium plates revealed scratches.
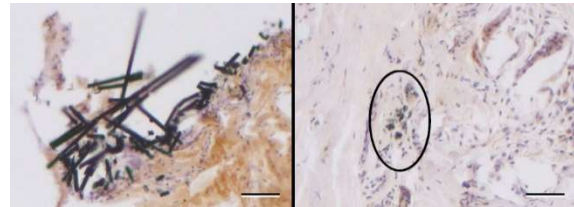

Fig. 1: Photos of histological sections of soft tissue next to CFR-PEEK plates (left) and titanium plates (right). On the left, large amounts of foreign bodies with rod-like and round configuration and significant tissue inflammation are evident. On the right, a few small foreign bodies (encircled) and less pronounced tissue inflammation are visible. Scale bars 50 μm.
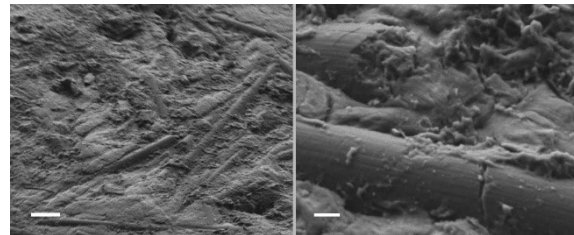

Fig. 2: At the surface of an explanted CFR-PEEK plate exposed and fractured carbon fibres are visible in scanning electron micrographs (scale bar left 10 μm, right 1 μm).

DISCUSSION & CONCLUSIONS: In the peri-implant tissue adjacent to CFR-PEEK plates, particles were observed in larger quantity compared to titanium plates. The inflammatory response was more distinct in the tissue adjacent to CFR-PEEK plates than to titanium plates. It could not be conclusively determined from which region of the implant the CFR-PEEK particles originated. However, looking at the implant characteristics, it is likely that they were released when the titanium screw heads were screwed into the holes of the CFR-PEEK plates.

In-silico implant validation: Establishing a reliable computational bone-implant model

M. Maintz[1,2,3], F. Dalcanale[1], D. Seiler[1], M. de Wild[1], FM. Thieringer[2,3]

[1]*University of Applied Sciences Northwestern Switzerland, FHNW, Muttenz, CH, [2]Medical Additive Manufacturing Research Group, Department of Biomedical Engineering, University of Basel, Allschwil, CH, [3]University Hospital Basel, Basel, CH*

INTRODUCTION: The correct surgical fracture fixation can be challenging as the unique patient-specific biomechanical circumstances are usually neither considered in the design process of the implants nor their positioning. Finite Element (FE) analysis is a computational method which is increasingly being used for the preoperative planning and design improvement of osteosynthesis plates because it can uncover regions of high biomechanically induced stresses in the bone, implant or its interface which are difficult to measure experimentally [1]. Adopting this *in-silico* testing method in the clinics can ultimately improve the treatment outcome as it would give the surgeon an indication of whether the treatment is suitable for the patient without the need to experimentally test the mechanical integrity. The challenge lies within establishing the reliability of the simulation, i.e., the "digital twin" of the patient. The result of the *in-silico* simulation is especially useful when the computational model has been previously verified and validated experimentally. Among facial bones, the lower jaw is often affected by fractures, which in many cases require the fixation with an implant [2]. In this study, the principle of validation of an *in-silico* mandible fracture model is demonstrated.

METHODS & RESULTS: The digital mandible model was obtained by segmentation of patient computed tomography (CT) data. The mandible models were then produced with Selective Laser Sintering of Polyamide 12. For the FE model, material properties (e.g. Young's modulus, Poisson's ratio) of the bone model, implant and screw material were determined. Material properties of bone can be derived from the CT Hounsfield unit value of the patient's bone. The contact definitions and material properties were optimized by comparing the intact mandible FE outcomes to the deformation behaviour of the experimental model of a biomechanical setup. A frictional

contact of $\mu = 0.1$ was chosen between the bone surface and the setup as well as between the implant and the bone. For biomechanical testing, a custom-made jig was used to apply a uniaxial load with a hydraulic testing machine to the mandibular angle region (Fig. 1). The stress-induced surface deformation was recorded with an optical scanning device capable of digital image correlation. Finally, the surface deformation and reaction force were statistically compared with the FE results and a high level of correlation was observed.
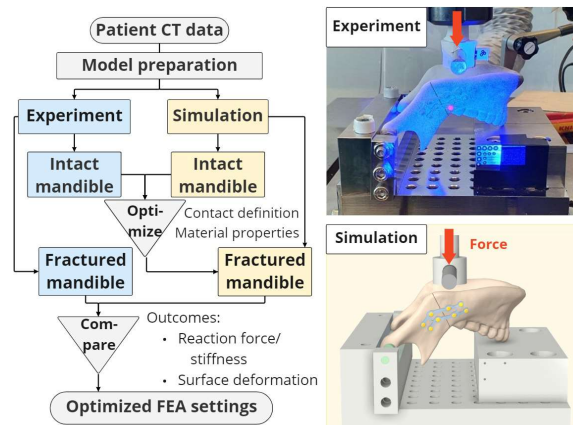

Figure 1 (left) Methodology of in-silico validation approach. (right) Depiction of the experimental setup and the CAD model for the FE analysis.

DISCUSSION: We proposed a workflow to virtually create a setup for mechanical bench testing of osteosynthesis plates on an additive-manufactured model of a patient's fractured jaw. We proved that the FE method can accurately depict mandibular fixation methods. With this method, patient anatomy and bone quality can be considered. The digital validation of implants can significantly speed up the process to bring effective osteosynthesis solutions to patients with time-critical traumatic injuries.

REFERENCES: [1]Lewis GS et al. Current osteoporosis reports. 2021:1-14. [2]Motamedi MHK et al. Journal of trauma and acute care surgery. 2014;77(4):630-4.

Making an impact:
In-vitro validation of operational strength of impact-loaded surgical instruments by means of an automated pendulum impact tester

R. Paul[1], M. Brensing[1], F. Herrmann[1], A. Klockow[2], F. Eitel[2]

[1]IMA Dresden, Dresden, DE, [2]Mathys Ltd Bettlach, Bettlach, CH

INTRODUCTION: Impact-loaded surgical instruments, e.g. hip cup positioners, are exposed to high forces at high loading rates. Validation of the operational strength of surgical instruments over their service life is becoming more important for product development and approval. The aim of this study was to establish a reproducible procedure to validate operational strength of such instruments.

METHODS: In a cadaveric study, the relevant forces and impulse time intervals were determined by a surgeon using an instrumented surgical hammer and a hip cup positioner. An identical hip cup positioner was tested in a specially constructed pendulum impact tester consisting of a striking element and pendulum arm with an adjustable deflection angle. Both the surgical hammer and the striking element were equipped with exactly the same piezo force transducer to determine the entry force over time.

Figure 1 shows the exemplary test setup: The entry force is shown by a red arrow (F_E) and the discharge force is illustrated by a blue arrow (F_D). The main parameters of the pendulum are defined by the length (l_P), mass (m_P) and angular deflection (α_P).
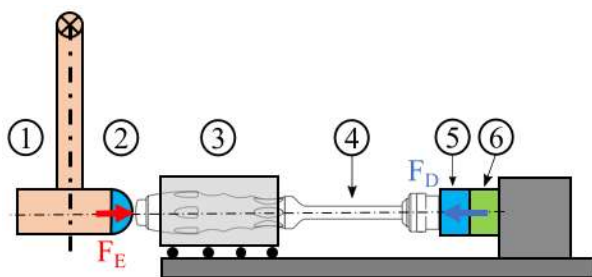

Figure 1: Exemplary setup of pendulum impact tester with pendulum (1), entry force transducer (2), instrument mounting fixture with linear bearing (3), surgical instrument (4), discharge force transducer (5), damping element (6).

RESULTS: The force amplitude of the surgeon's impacts varied during the hip cup impaction with an average force amplitude of 20.24 ± 7.35 kN. Therefore the deflection angle of the pendulum impact tester was adjusted to generate the average force amplitude of the surgeon.

Table 1: Comparison of impact signals from cadaveric study and pendulum impact tester regarding force amplitude and impulse interval duration.

Parameter	Cadaveric study (n=23)	Impact tester (n=36)
Average force amplitude [N]	20'240 ± 7'345	19'954 ± 345
Average impulse interval [µs]	260 ± 114	161 ± 15

DISCUSSION & CONCLUSIONS: The averaged intraoperative impact on the investigated hip cup positioner could be well reproduced by means of the pendulum impact tester. The authors believe that cyclic pendulum impact testing makes a valuable contribution to the validation of the operational strength of impact-loaded surgical instruments over their respective service life as well as contribute to the development and approval process of new instruments. This method may be applied to other kinds of insertion instruments of different geometry and averaged force amplitude.

Authors, Program Committee

Participant	Company Name	Location	E-Mail	Function
Dr. Oksana Banakh	University of Applied Sciences of Western Switzerland (Haute Ecole Arc)	2300 La Chaux-de-Fonds, Switzerland	oksana.banakh@he-arc.ch	Speaker, Session 3
Dr. Simon Berner	Medicoat AG	5506 Mägenwil, Switzerland	s.berner@medicoat.ch	Program Committee
Matthias Brensing	IMA Materialforschung und Anwendungstechnik GmbH	01099 Dresden, Germany	Matthias.Brensing@ima-dresden.de	Poster presenter 7
Prof. Dr. Michael de Wild	FHNW	4132 Muttenz, Switzerland	michael.dewild@fhnw.ch	Program Committee
Dr. Lukas Eschbach	RMS Foundation	2544 Bettlach, Switzerland	lukas.eschbach@rms-foundation.ch	Program Committee / Main Organizer
Sophie Farine	University of Applied Sciences of Western Switzerland (Haute Ecole Arc)	2300 La Chaux-de-Fonds, Switzerland	sophie.farinebrunner@he-arc.ch	Poster presenter 4
Harald Holeczek	Medicoat AG	5506 Mägenwil, Switzerland	h.holeczek@medicoat.ch	Speaker, Session 3
PD Dr. habil. Christiane Jung	KKS Ultraschall AG	6422 Steinen, Switzerland	christiane.jung@kks-ultraschall.ch	Program Committee
Dr. Dmitrii Komissarenko	EMPA - Swiss Federal Laboratories For Materials Science and Technology	8600 Dübendorf, Switzerland	dmitrii.komissarenko@empa.ch	Speaker, Session 2
Martin Liebelt	Mathys Orthopaedie GmbH	7646 Moersdorf, Germany	martin.liebelt@mathysmedical.com	Speaker, Session 2
Michaela Maintz	FHNW	4123 Muttenz, Switzerland	michaela.maintz@fhnw.ch	Poster presenter 6
PD Dr. med. Dr. phil. Andrej M. Nowakowski	Kantonsspital Baselland	4101 Bruderholz, Switzerland	andrej.nowakowski@ksbl.ch	Keynote Speaker, Session 4
Erik Poulsen	GF Machining Solutions	2504 Biel, Switzerland	erik.poulsen@georgfischer.com	Poster presenter 1
Dr. Samuel Rey-Mermet	HES-SO Valais	1950 Sion, Switzerland	samuel.rey-mermet@hevs.ch	Speaker, Session 3
Dr. Sanja Savic	OFI Technologie & Innovation GmbH	1030 Vienna, Austria	sanja.savic@ofi.at	Speaker, Session 4
Dr. Hans Schmotzer	SigmaRC GmbH	6330 Cham, Switzerland	hans.schmotzer@sigma-rc.com	Speaker, Session 4
Christian Söhner	FOBA Laser Marking + Engraving	ALLTEC Angewandte Laserlicht Technologie GmbH	23923 Selmsdorf, Germany	christian.soehner@fobalaser.com	Poster presenter 2
Christoph Sprecher	AO Research Institute	7270 Davos, Switzerland	christoph.sprecher@aofoundation.org	Speaker, Session 4, Poster presenter 5
Dr. Martin Stöckli	inspire AG	8005 Zürich, Switzerlanc	stoeckli@inspire.ethz.ch	Program Committee
Dr. Juliane Thielsch	Fraunhofer Institute for Machine Tools and Forming Technology IWU	01187 Dresden, Germany	juliane.thielsch@iwu.fraunhofer.de	Speaker, Session 2
PD Dr. med. et med. dent. Florian M. Thieringer	Universitätsspital Basel	4031 Basel, Switzerland	florian.thieringer@usb.ch	Keynote Speaker, Session 2
Dr. Dieter Ulrich	Helbling Technik	3097 Liebefeld-Bern, Switzerland	dieter.ulrich@helbling.ch	Speaker, Session 3
Prof. Dr. Konrad Wegener	ETH Zürich, LEE L 214	8092 Zürich, Switzerland	wegener@iwf.mavt.ethz.ch	Keynote Speaker, Session 1
Jürgen Wuttig	Sauber Technologies AG	8340 Hinwil, Switzerland	juergen.wuttig@sauber-group.com	Speaker, Session 2
Helen Yau	Koln 3D Switzerland	1209 Geneva, Switzerland	helen@koln3d.ch	Speaker, Session 4
Janick Zehnder	FHNW	4123 Muttenz, Switzerland	janick.zeh@gmail.com	Poster presenter 3

Notes

Notes

Notes
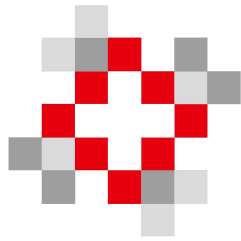
SWISS MEDTECH EXPO

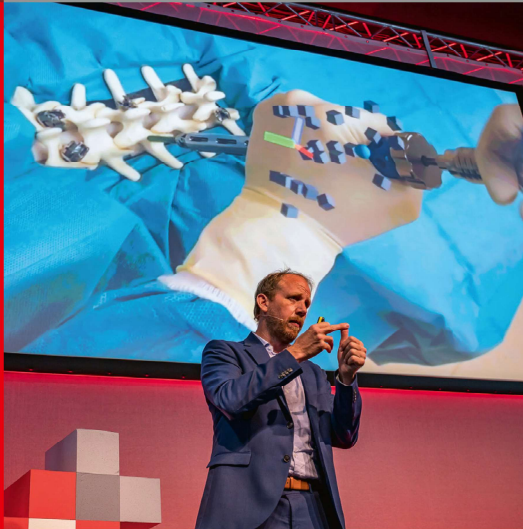**The high-caliber meeting place for the industry**
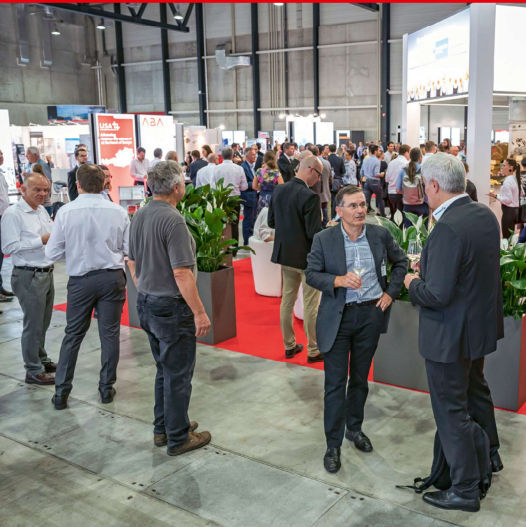
September 12 to 13 2023

Messe Luzern

Save the date

AMX
Additive Manufacturing Expo

Takes place in parallel

medtech-expo.ch

Industry partners

HEALTH TECH CLUSTER SWITZERLAND

SWISS MEDTECH

Organizer

MESSELUZERN